Journal of Radiation and Nuclear Applications
An International Journal

http://dx.doi.org/10.18576/jrna/040201

Correlation between the Build-up Factor, the γ-ray Energy and the Effective Atomic Number in Open-Angle Measurements

A.H. El-Kateb[*]

Faculty of Science, Helwan University, P. Nr. 11792, Helwan, Cairo, Egypt.

Received: 3 Mar. 2018, Revised: 12 Apr. 2019, Accepted: 27 Apr. 2019.
Published online: 1 May 2019.

Abstract: The spectra of γ-rays attenuated by soil, water, sand and cement in a broad beam geometry have been measured and analyzed at the energies 0.662 MeV from ^{137}Cs and 1.173, 1.333 MeV from ^{60}Co. The ratios of the photopeak to four main portions of the spectra were analyzed as a function of the material effective atomic number Z_{eff} and the γ-ray energy. The broad beam mass attenuation coefficients μ_b/ρ were compared with the theoretical values μ/ρ as a function of the effective atomic number Z_{eff} and γ-ray energy. The photopeak ratios have maximum values for photons scattered in the forward directions and decrease gradually for larger scattering angles. An inversion trend IT (maximum intensity build-up) in the peak ratios as a function of γ-ray energy holds, in agreement with earlier results, where a decrease at the energy region 0.662 to 1.173 MeV changes to an increase at the energy region 1.173 to 1.332 MeV. These trends vanish gradually at larger scattering angles. The build-up factor B decreases with increase in the γ-ray energy. Correlation between the build-up factor B and each of the effective atomic number Z_{eff} and the γ-ray energy was registered and discussed. Extensive attention to preparing collimated beam to measure μ/ρ might be saved if the measurement is performed under the conditions of minimum build-up factor B (maximum photopeak ratios).

Keywords: Gamma-ray spectrometry, Mass attenuation coefficients, Peak ratios, Effective atomic numbers, Build-up factor.

1 Introduction

On passing through the material, γ- rays undergo attenuation because of their interaction with the material atoms. This interaction depends on the γ-ray energy, the material atomic number, and the experimental set-up. The mass attenuation coefficient μ/ρ is a measure of the probability of interaction between incident X- or γ- rays and the sample atoms. The accurate values of μ/ρ are required to provide data in diverse fields. Investigation for measuring μ/ρ was performed to gain shielding data for the constituents of concrete in the γ-ray energy range of 0.662 to 1.332 MeV. It was concluded that beach soil is the best sand type for making concrete of ionizing radiation shielding [1]. The 33, 662, 1173 and 1332-keV γ-rays were employed as single and dual-energy broad beams to study the attenuation of applied mixed materials. It was concluded that soft X-rays, 33- keV as a single energy and 33-1250 keV as dual-energy produce the most sensitive responses to concentrations [2]. The main processes of interactions are absorption, scattering (single or multiple), emission of fluorescence radiation, the annihilation of positrons, generation of bremsstrahlung which give rise to secondary photons that are evaluated through a build-up factor [3]. It simply compares between the intensity of the photons at a certain point with the collisions to the intensity without collisions at the same point, therefore its minimum value is one. The arrangement is an open angle and broad beam geometry mostly applied in the environmental, dosimetric, shielding, radiotherapy, mining studies. The mass attenuation coefficients μ/ρ and the mean free path λ are directly affected by the build-up in the intensity so that μ/ρ becomes smaller than the theoretical values and λ becomes larger. The background under the peak, the Compton valley, and the Compton plateau correspond to different scattering angles and can be utilized to be compared with the photopeak. The peak-to-valley ratios for three different HPGe detectors were measured for the assessment of ^{137}Cs deposition on the ground and the impact of the detector field-of-view [4]. This is necessary for the problem of quantification of the total deposition of radioactivity after the release of radioactive material to the environment. Broad beam γ-ray spectra were studied before and after passing through vital materials and the variations

[*]Corresponding author e-mail: elkateb@hotmail.com

in the photo peak ratios to different parts in the spectra besides measuring μ_b/ρ at the three energies 0.662, 1.25 and 1.332 MeV [5]. The photopeak ratios to the forward scattering parts in the spectra revealed inversion trend, IT, from decrease at 0.662-1.25 MeV region to increase at 1.25-1.332 MeV region. Properties of environmental, biological, industrial materials are often evaluated and compared against each other by consideration to Z_{eff}. This method was applied, on water and dosimetric gels [6]. Broadening of the peaks can be caused by overlapping of peaks of nearby energies either from the same isotope or from another one, besides the increase in the back ground. Fitting algorithms are used to analyze this overlap to determine physical quantities as for example the specific activity of ^{137}Cs in a radioactive material [7]. Determination of γ-ray spectrometric parameters e.g. the effective atomic numbers, the effective electron numbers, the total atomic cross-sections and build-up factor of some compounds and some building materials at different γ-energies was performed in [8,9]. It was reported that an increase in the beam collimator diameter causes increases in the build-up factor [8].
In the present work the attention is directed to:

1- Investigate the development of γ-ray spectra in an open angle geometry where the material is put between the source and the detector.
2- Verify the existence of minima in the ratios of the photopeak to selected regions of the attenuated γ-ray spectra at the energy interval 0.662-1.332 MeV [5].
3- Measure the broad beam mass attenuation coefficients μ_b/ρ and compare them with the theoretical values μ/ρ.
4- Correlate between the build-up factor B, the effective atomic number Z_{eff} and the γ-ray energy E_γ.

2 Experimental Section

2.1 Theoretical Background

The dominant mode of interaction at the energies applied is the Compton scattering. An overview of the contributions of interactions for the atomic number Z=8 (oxygen) and Z=13 (aluminum) indicates that the ratio of photoelectric interaction to the Compton interaction ranges between 10^{-2} and 10^{-3}. The ratio of pair production to Compton scattering at 1.173 and 1.333 MeV is of the order 10^{-3} [10]. The energy loss in one collision depends on the γ-ray energy E_γ and the scattering angle θ according to the relation,

$$E = \frac{E_0}{1 + \left(E_0/m_0 c^2\right)(1 - \cos\theta)} \quad (1)$$

E_0 and E represent the γ-ray energy before and after scattering at an angle θ and $m_0 c^2$ is the rest mass energy of the electron. The differential scattering cross section $d\sigma(E.\theta)/d\Omega$ depends on the energy and the angle of scattering according to the Klein- Nishina formula,

$$d\sigma(E.\theta)/d\Omega = \frac{r_0^2}{2}\left(\frac{E}{E_0}\right)^2\left[\left(\frac{E}{E_0}\right) + \left(\frac{E_0}{E}\right) - \sin^2\theta\right] \quad (2)$$

r_0 is the classical electron radius. dΩ represents the solid angle corresponding to the scattering angle θ. This equation shows no dependence on the atomic number Z or the density ρ of the attenuator, however, the Compton cross section is proportional to Z. According to [11], the number of scattered photons is proportional to each of the scattering angle and the thickness of the attenuator. Therefore, the Compton continuum occurs in the energy spectrum of the attenuated photons, depending on the Z number and the γ-ray energy. A build-up factor B, (with minimum value ≅1) was developed to quantify this quantity from comparison with the forwardly scattered photons in a parallel (narrow) beam geometry, according to the relation $B = \frac{I_{measured}}{I_{calculated}}$, where $I_{measured}$ represents the measured intensity from the broad beam geometry and $I_{calculated}$ represents the corresponding measured intensity from a parallel beam geometry. The build-up factor B relates the narrow (theoretical) beam to broad beam mass attenuation coefficients as follows,

$$I_{measured} = B\, I_{calculated}\, e^{-\left(\frac{\mu}{\rho}\right)t} \quad (3)$$

$$B = e^{[(\mu/\rho) - (\mu_b/\rho)]t} \quad (4)$$

t is the material thickness.
A basic quantity related to μ/ρ is the effective atomic number Z_{eff}. It is used to describe the properties of a composite material in terms of its constituents. General expressions have been obtained for the description of effective atomic number Z_{eff} [12].

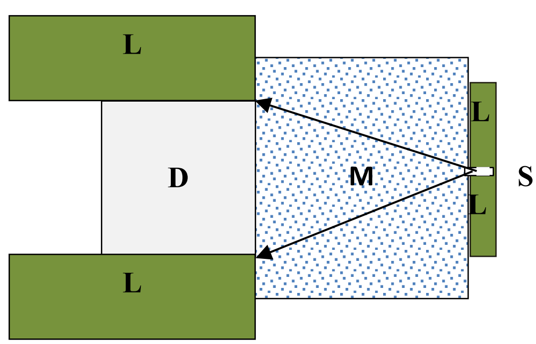

Fig.1: Schematic diagram of the experimental set-up. D: Detector, L: Lead shield, M: Material, S: γ-ray source.

The sources used are ^{137}Cs and ^{60}Co of activities 580 and 180 μCi respectively. The γ-ray spectra were measured using 3″x3″ NaI (Tl) detector. The attenuator was packed in a plastic container with thickness 14 cm and mounted in contact between the source and detector in an open angle geometry. Using the definition, $\lambda_{th} = 1/\mu_{th}$, the thickness 14 cm of water is equivalent to 1.2 times the theoretical mean free path, mfp, λ_{th} at E_γ= 0.662 MeV and is equivalent only to 0.910 and 0.86 times Its value at E_γ=1.173 and 1.332 MeV respectively. The densities for water, soil, cement, and sand are respectively 1, 1.33, 1.44 and 1.74 g cm^{-3}. The γ-ray source was enclosed in a lead shield with a pin hole on the side facing the detector. The acceptance angle at the detector is 15.34^0 and the corresponding solid angle= 0.64 sr. Figure 1 shows a schematic diagram of the experimental set-up. The detector resolution is 7.8% for 0.662 MeV and 5.3% for 1.173, 1.332 MeV photons. The peak to Compton ratio as well as the resolution specification are presumably reasonable. The size of the active cone in the material= 201 cm^3. The sizes of the active cone (cone tractors) based on the experimental geometries in [5] are 12.52, 154 and 527.12 cm^3. Additionally, the sum peak of energy 1.25 MeV (representing the two cascade of energies 1.173 and 1.332 MeV in the decay scheme of ^{60}Co is replaced in this study by the peak of 1.173 MeV photons.

The photopeak was compared with:

- i) The background in its region to get the peak to back ground ratio, PtBG.
- ii) The sum of the photopeak plus background in its region to get the peak to total ratio PtT.
- iii) A nominated energy range in the Compton valley to get the PtV ratio.
- iv) A nominated energy range in the Compton plateau to get the PtC ratio.

The regions of interest are normalized to allow comparisons and evaluations.

Table 1: Regions of interest, ROI for the peak ratios.

E_γ (MeV)	Photopeak (MeV)	Valley (MeV)	Plateau (MeV)
0.662	0.566-0.766	0.500- 0.548	0.218- 0.266
1.173	1.082- 1.256	1.025- 1.17	0.650-0.811
1.332	1.241-1.460	1.025- 1.170	0.650- 0.811

Table 1 lists the energies of regions of interest. The peak ratios obtained from the number of counts per channel per second were calculated to verify behaviors of the peak ratios obtained from the regions of interest. The peak centroids for the attenuators are close to each energy but quite shifted from the corresponding backgrounds because of photon energy loss ΔE_γ, which is~ 0.04 MeV at E_γ= 0.662 MeV and~ 0.023 MeV at the two energies 1.173, 1.332 MeV. The broad beam mass attenuation coefficients μ_b/ρ were measured and illustrated in Fig. 1.

Table 2: The effective atomic numbers for the attenuators [12-15].

Attenuator	Photo electric effect	Compton	Pair production
Water	7.98	7.22	7.89
Soil	12.77	12.77	12.77
Cement	15.7	13.65	14
Sand	12.3	10.8	11.63

The theoretical values of the mass attenuation coefficient μ/ρ were calculated using the chemical compositions in [12-15] and XCOM program [10]. The effective atomic numbers Z_{eff} were calculated according to the expressions given by [12] and the chemical compositions from [13-15]. Table 2 lists the values of effective atomic number Z_{eff}. The build-up factor B was calculated using μ/ρ, μ_b/ρ and equation 4, see table 3.

The errors in μ_b/ρ have been calculated from the propagation of errors according to the relation given in [8].

$$\Delta\left({}^{\mu_b}/_{\rho}\right) = \left(-{}^{1}/_{\rho\, t}\right)\left\{[(I\,\Delta I_0 - I_0\,\Delta I)/II_0] + t\Delta\rho \ln\left(\frac{I}{I_0}\right)\right\} \quad (5)$$

where t is the container thickness, I_0 and I are the numbers of counts without and with the material, the errors from typical cases are less than 6%.

3 Results and Discussion

3.1 Peak ratios as a Function of Effective Atomic Numbers

Generally, the peak ratios results are inversely proportional to the E_γ and Z_{eff}. The relatively large source-detector solid angle Ω allows prevailing Compton continuum to be achieved by the detector. Consequently, it was necessary to choose small ROI which yielded large values of PtV and PtC.

This paragraph is the caption of figures 2. It has to be moved to be directly below figures 2A,2B,….., 2E as a function of Z_{eff}. The inversion trend, IT reported in [5], takes place where the PtT ratios for the energy 1.332 have values near the values of 0.662 MeV and larger than the 1.173 MeV values. For each group

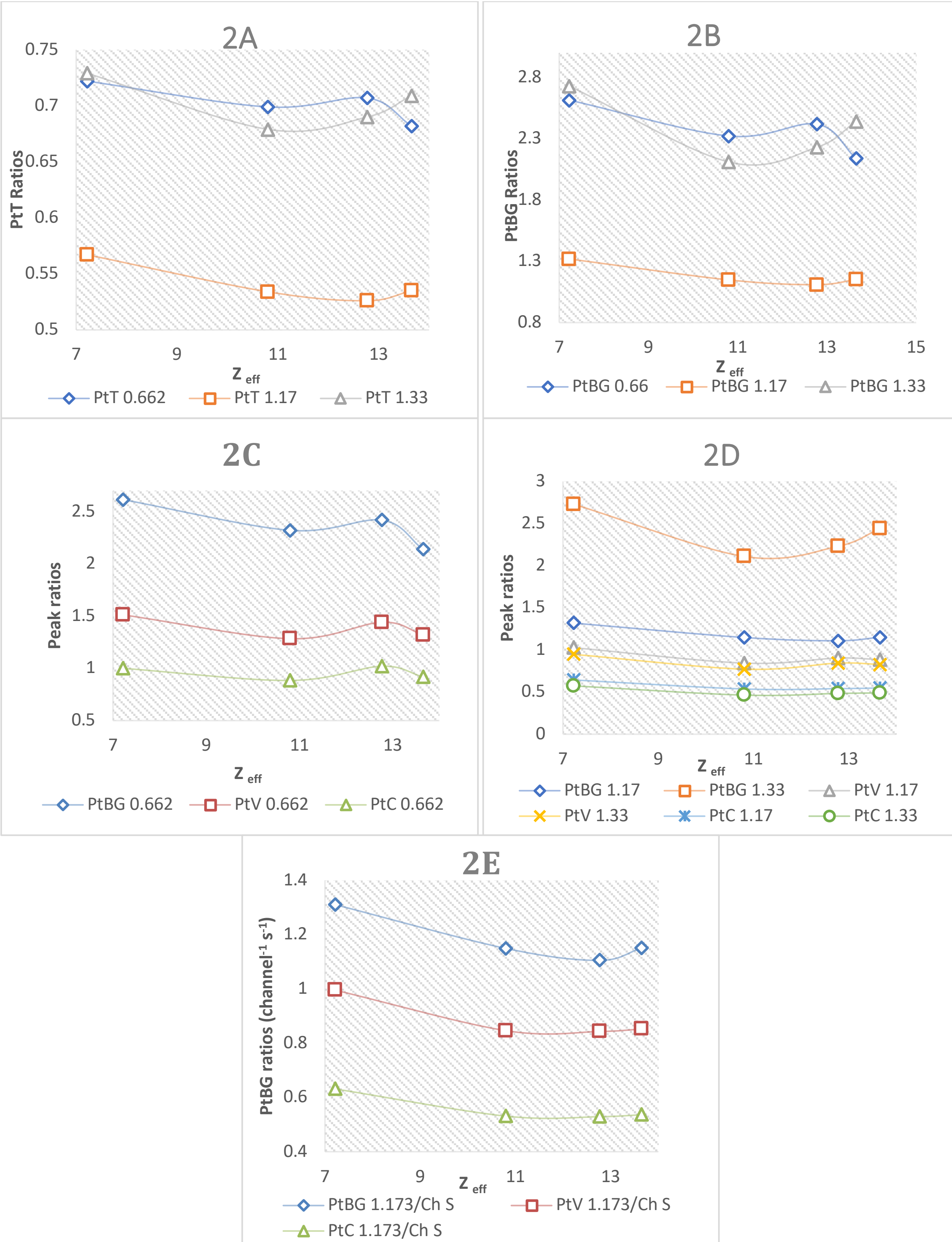

Fig. 2: A the PtT ratios for the three energies 0.662, 1.173 and 1.332 MeV as a function of Z_{eff}. B PtBG ratios for the three energies 0.662, 1.173 and 1.332 MeV as a function of Z_{eff}. C Peak ratios for the energy 0.662 MeV as a function of Z_{eff}. D Peak ratios for the energies 1.173 and 1.332 MeV as a function of Z_{eff}. E Peak ratios per (channel second) at the energy 1.173 MeV as a function of Z_{eff}.

of photons, both transfer and absorption of energy occur. The net result is that the accumulated energy transferred initially builds-up with depth to a maximum value and then decreases by absorption. The maximum build-up corresponding to 1.173 MeV exceeds the maxima at 0.662 and 1.332 MeV. The single (forward) scattering produces the main contribution in the background under the photopeak. In Figure 2B, the PtBG plots are ordered systematically as occurred in the PtT plots shown in Figure 2A but with larger ratios. In Figure 2C the multiple scattering let the Compton continuum grows-up, correspondingly the peak ratios for 0.662 MeV decrease from PtBG to PtV to PtC. According to Klein-Nishina formula 2, the differential scattering cross section is subjected to decrease with larger scattering angles and increase in γ-ray energy. According to Figure 2D the peak ratios are more divergent with respect to Z_{eff} at 1.332 MeV than 1.173 MeV. From the measured spectrum, the intensity in the peak plus background at 1.173 MeV is larger than at 1.332 MeV owing to an increase in the Compton continuum but the background in 1.173 MeV is relatively higher than at 1.332 MeV. Consequently, the ratios PtBG at 1.332 MeV are larger than at 1.173 MeV, this is not the case for the PtV and PtC ratios. Irrespective of the build-up effect, from comparison with the XCOM calculations [10], the ratio of Compton cross sections at 1.173 MeV to 1.332 MeV for soil as an example= 0.937. Similar results are found in [3], the shield Kernel B (μ r) exp (-μ r) in infinite water has maximum values (inversion tends) as a function of the distance from the source for γ-ray energies between 0.03 and 0.3 MeV. The greatest shield Kernel was registered at 0.08 MeV. The results are analyzed from another point of view, Figure 2E illustrates the peak ratios for the γ-ray energy 1.173 MeV according to the counts per (channel second) in the photopeak, valley and Compton regions at the energy 1.173 MeV. It shows that PtBG> PtV> PtC, which agrees with the sequences shown in Figures 2C- 2D. This leads to understanding that the IT is a matter of the scattering angle because it is the unique varying parameter in the set of data.

3.2 Peak Ratios as a Function of Energy

Despite a quite variation with the same rate occurs between the PtV and PtC, in the Z_{eff} versus peak ratios plots, more details concerning the ratios are derived from the plots of peak ratios versus energy. It is worth to note that the smooth curve of the detector efficiency shown in given by [16] does not play a role in IT.

Figure 3A shows the PtT ratios for the background and the attenuators as a function of energy, the plots decrease from 0.662 to 1.173 MeV and increase from 1.173 MeV to 1.33 MeV. The ratios indicate to a sensitivity of the build-up at 0.662 MeV where the ratios are distant from each other and are approached at 1.173 and 1.332 MeV. Figure 3B shows the PtBG, PtV, and PtC ratios for all attenuators. Figure 3C shows the features of the photopeak ratios for water. The ratios PtBG display the IT where the values at 1.33 MeV are clearly larger than at 1.173 MeV, which is not the case in the PtV and PtC ratios. The increase with respect to the Z_{eff} (and Z) holds most clearly in the PtBG ratios. The PtV and PtC ratios, on the other hand, show no clear IT, this is attributed to the significant increase in the Compton continuum at larger scattering angles and not to Z_{eff}.

3.3 Mass Attenuation Coefficients

The chemical composition of the materials [13-15] was employed to determine the theoretical mass attenuation coefficients μ/ρ using XCOM program [10].

Figures 4A and 4B show respectively μ_b/ρ and μ/ρ as a function of Z_{eff}. The theoretical plots show similar trends at the three energies, the broad beam plots, on the other hand, show maximum at cement with the γ-ray energies 1.173 and 1.332 MeV which is not the case at E_γ= 0.662 MeV. This result agrees with the minima in PtT and PtBG ratios found in Figures 2A and 2B at the γ-ray energy 1.173 MeV. The relative attenuation of photons by the photoelectric absorption to incoherent scattering does not exceed few 10^{-2}-10^{-3}, for the materials and energies under study. One can correspondingly think of prevailing Compton continuum in the spectral variations under study. The larger Z materials generate more build-up photons causing decrease in μ/ρ side by side with photon removal from reaching the detector till some sort of saturation is attained at a Z_{eff} of about 12.7. The mean free paths λ in broad beam geometry are respectively λ_b= (1/μ_b) =12.53 and 13.67 cm for the 1.173 and 1.332 MeV photons passing in soil. Figures 4C and 4D show respectively μ_b/ρ and μ/ρ as a function of γ-ray energy. The γ-ray build-up causes the rates of decrease of μ_b/ρ with respect to E_γ to be varying more than μ/ρ. In this respect, it should be mentioned that the scattering angle θ is constant in this case.

3.4 Build-up Factor

The build-up factor B= e[(μ/ρ) -(μ b/ρ)]t, Equation 4, represents the capability of attenuation by the material. The build-up factor B has been calculated from the values of the mass attenuation coefficients given above (μ/ρ from XCOM program and μ_b/ρ from present work). The values of B are listed in table 3. B has largest values at the γ-ray energy 0.662 MeV and smaller values at higher energies in accordance with Klein-Nishina formula where the differential scattering cross section (for certain scattering angle θ), increases appreciably with decrease in incident photon energy, consequently, μ_b/ρ is decreased [17]. The theoretical values at soil, cement and sand coincide and the value for water is larger, the build-up on the other hand folds the μ_b/ρ for the different materials besides reducing their values.

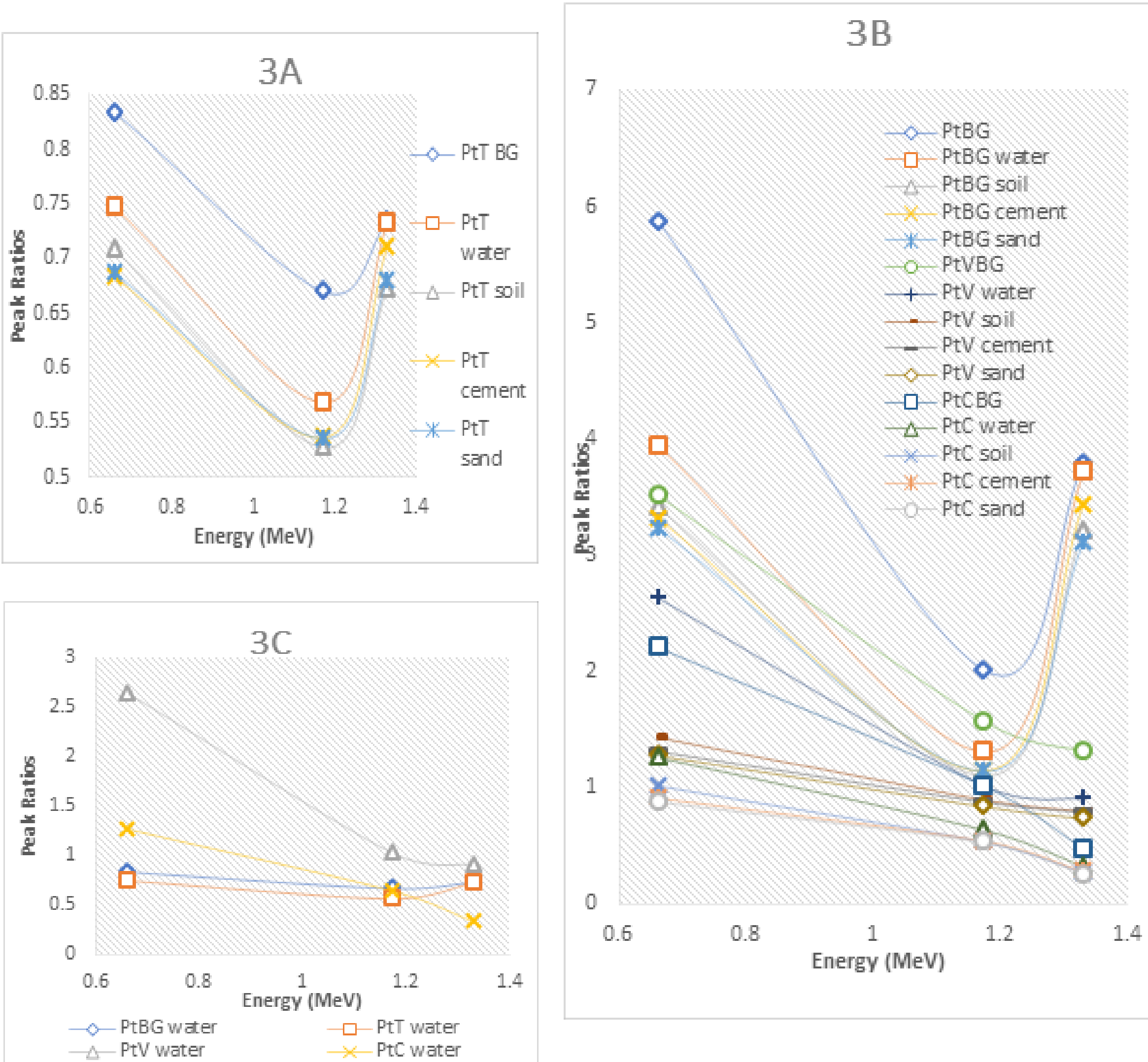

Fig. 3: A the PtT ratios for all materials as a function of γ-ray energy. B Peak ratios for all materials as a function of γ-ray energy. C Peak ratios for water as a function of γ-ray energy.

Table 3: The build-up factor according to the present study.

E_γ (MeV)	B_{Water}	B_{Soil}	B_{Cement}	B_{Sand}
0.662	1.394	1.322	1.237	1.186
1.173	1.124	1.135	1.051	0.982
1.332	1.237	1.081	0.999	1.044

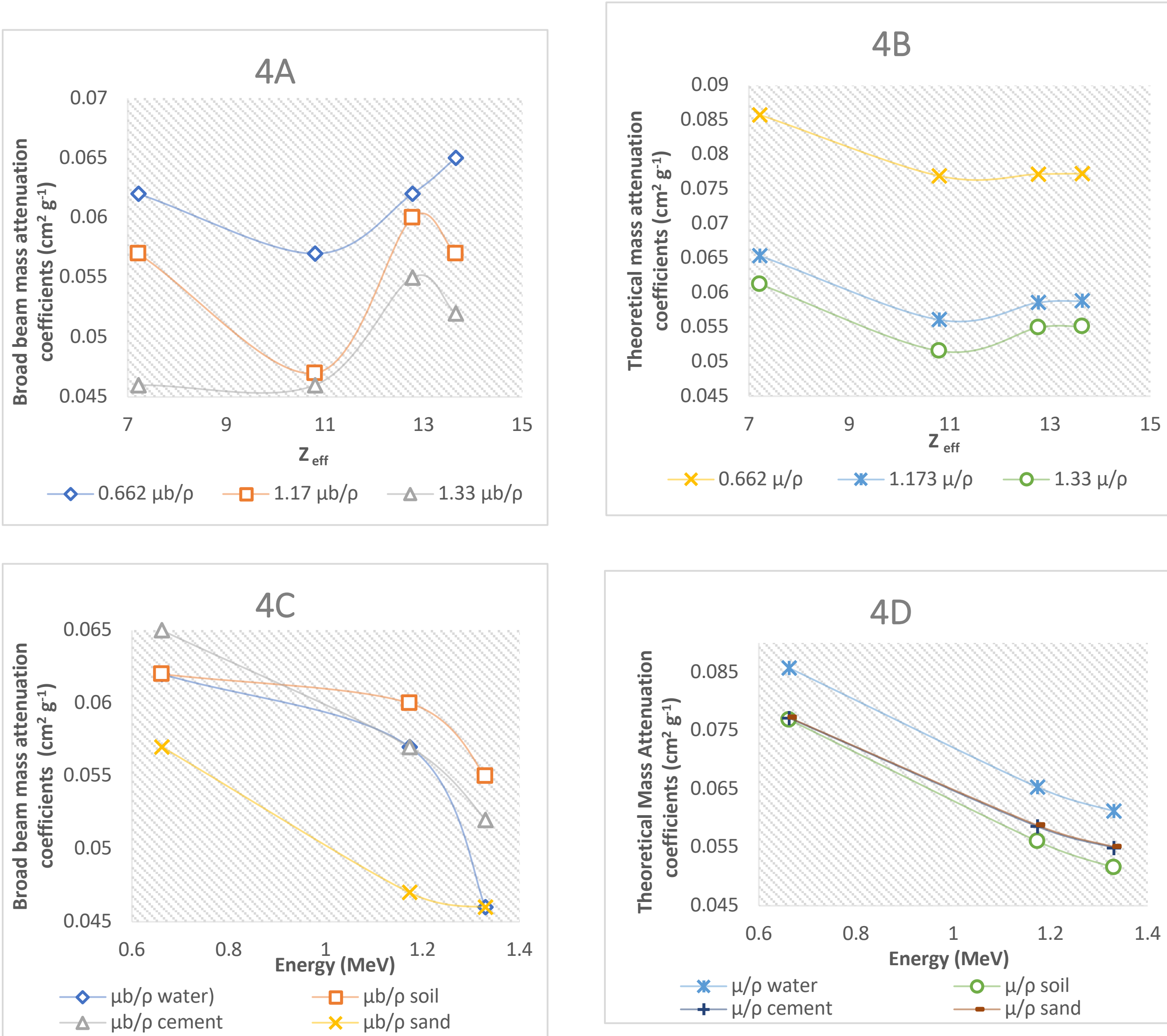

Fig.4:A the broad beam mass attenuation μ_b/ρ as a function of Z_{eff}. B the theoretical mass attenuation μ/ρ as a function of Z_{eff}. C the broad mass attenuation μ_b/ρ as a function of γ-ray energy. D the theoretical mass attenuation μ/ρ as a function of γ-ray energy.

4 Conclusions

The present results provide contribution to the open field measurements as the environmental, shielding, dosimetric, and mining studies. The PtT and PtBG ratios correspond to forward scattering while the PtV and PtC ratios correspond to increasing scattering angles. Comparison between the ratios at the three energies 0.662, 1.173 and 1.332 MeV let it be concluded that PtT and PtBG ratios are the largest sensitive to variations in the experimental conditions, (geometry, attenuator properties, gamma-ray energies etc). The ratios are inverted from decrease at the region of energy 0.662- 1.173 MeV to increase at the region 1.173-1.332 MeV. This trend gradually disappears at the PtV and PtC ratios. From the results of μ/ρ and μ_b/ρ the intensity build-up is maximum at lower γ-ray energy and lower Z_{eff} material. At the energies 1.173 and 1.332 MeV μ_b/ρ are maximum (B is minimum) with Z_{eff}= 12.5. Extensive attention to prepare collimated beam to measure μ/ρ and determine γ-ray spectrometric parameters might be saved if the dimensions of the experimental set-up, the photon energy and the material characterization are chosen so that B is minimum. This corresponds to the conditions of maximum photopeak ratios. In in-situ measurements, on the other hand, large intensity is demanded, and the experimental set-up is suggested to match with the inversion trend, IT.

Acknowledgement: The author would like to thank, the Physics Department in Helwan university to provide the facilities to perform the resent work.

References

[1] F.O. Ogundare, S.A. Ogundele, O.O. Akerele and F.A. Balogunm, Low-energy broad-beam photon shielding data for constituents of concrete, J. of Appl. Clinic. Med. Physics .,**13(2)**,176-182, 2012.

[2] A.H. El-Kateb, Semi-broad beam gamma spectrometry of some mixtures and solutions, Nucl. Sci. Eng., **134(1)**, 97-105, 2000.

[3] Y. Harima and S. Tanaka, A study of build-up factor, angular and energy distribution of small distances from three source geometries- plane isotropic, point isotropic and plane normal for low-energy gamma-ray incidence on water, Nucl. Sci. and Eng ., **90(2)**,165-173,1985.

[4] K. Östlund C. Samulson S. Matsson and C.L. Raaf, Peak-to-valley ratios for three different HPGe detectors for the assessment of 137Cs deposition on the ground and the impact of the detector field-of-view, Appl. Radiat. Isot., **120**, 89-94, 2017.

[5] A.H. El-Kateb, Broad beam gamma ray spectrometric studies with environmental materials, J. Radiat. Protec. and Research, **43 (2)**, 75-84, 2018.

[6] M.L. Taylor and R.D. Franich, J.V. Trapp, The effective atomic number of dosimetric gels, Australian physical and engineering sciences in medicine, Technical note, **31(2)**, 131-137, 2008.

[7] L.L. Zhang, N. P. Wang, B.C. Li., Extraction of full energy peak of 137Cs from in-situ NaI (Tl) gamma-ray spectrum, Nucl. Sci. Technol., **84**, 83-89, 2016. DOI:

[8] A. H. El-Kateb and Abdul-Hamid, Photon attenuation coefficient study of some materials containing hydrogen, carbon and oxygen, I. Radia. Appl. Instrum. Part A., **42(3)**, 303-307, 1991.

[9] K. S. Mann, M. S. Heer and A. Rani, A comparative study of gamma-ray interaction and absorption in some building materials using Zeff- toolkit, Rad. Effects and Defects in Solids., **171**, 7-8, 2016.

[10] M.J. Berger and J.H. Hubbell. XCOM Web Version 1.2, National Institute of Standards and Technology, Gaithersburg, MD, 1999; 20899-8460, USA. Originally published as XCOM photon cross section on a personal computer. NBSIR87-3597 (1987/1999).

[11] G.S. Sidho, A. Kumar G.S. Mudahar, Simultaneous effect of collimator size and absorber thickness on the γ-ray build-up factor, Indian J. Pure Appl. Phys., **42(7)**, 475-478, 2004.

[12] S.V. Naydenov, V.D. Ryzhikov, C.F. Smith, Direct reconstruction of the effective atomic number of materials by the method of multi-energy radiography, Nucl. Instr. Methods., **B215(3-4)**, 552-560, 2004.

[13] M. Kurudirek, M. Aygun and S. Z. Erzeneoglu, Chemical composition, effective atomic number and electron density study of trommel sieve waste (TSW), portland cement, lime, pointing and their admixtures with TSW in different proportions, Appl. Radiat. Isot., **68 (6)**, 1006-1011, 2010.

[14] G. Mudahar, S. Modi, S. Makhan, Total and partial mass attenuation coefficients of soil as a function of chemical composition, Appl. Radiat. Isot ., **42(1)**, 13-18,1991.

[15] K. Bala and R. Khan. Leonardo, Characterization of beach/river sand for foundry application, Journal of Sciences, Issue23, July-December., **(23)**, 77-83, 2013.

[16] I. Akkurt, K. Gunoglu, S.S. Arda, Detection efficiency of NaI (Tl) detector in 511- 1332 keV energy range, Science and technology of nuclear installation, 2014. Article IDo186798, 1-5 2014. http://dx.doi.org/10.1155/2014/186798

[17] G.E. Knoll, Radiation Detection and Measurement, John Willey and sons, New York, 3rd edition., 52, 2000.